MM Science Journal | www.mmscience.eu
ISSN 1803-1269 (Print) | ISSN 1805-0476 (On-line)
Special Issue | HSM 2025
18th International Conference on High Speed Machining
October 15-16, 2025, Metz, France
DOI: 10.17973/MMSJ.2026_06_2025099

HSM2025-44742

POCKET MILLING ON THIN SLENDER ALUMINIUM 5083 WORKPIECES UNDER UNIFORM BENDING LOADS

A. Sainz de la Maza Garcia[1]*, L. N. Lopez de Lacalle Marcaide[1], G. Martinez de Pisson Caruncho[1]

[1]Aeronautics Advanced Manufacturing Centre (CFAA), University of the Basque Country (UPV-EHU), Zamudio, Spain

*Corresponding author; e-mail: alvaro.sainzdelamaza@ehu.eus

Abstract
In milling, one of the main concerns is the tendency of introducing high magnitude tensile residual stresses in the machined surface, very harmful against fatigue. To assure a high surface integrity without postprocessing operations, a new approach is proposed: milling under an externally applied bending load. This article presents a simple fixture design to efficiently achieve this objective, and the experimental validation of the introduced residual stresses using this method limited to the analysis of pocket milling operations in aluminium alloy. This research showed positive results introducing compressive residual stresses and reducing cutting forces during milling using the proposed fixture.

Keywords:
Prestress Assisted Machining, milling, residual stress, pocket, fixture

1 INTRODUCTION

Milling is one of the most used manufacturing technologies, particularly when workpiece geometry is complex. Thus, many components on mechanical systems are manufactured using this method. Critical mechanical components are often subjected to cyclical mechanical or thermal loads, promoting crack propagation and as a consequence, fatigue failure.

Fatigue commonly starts in the vicinities of surface defects. Therefore, fatigue crack growth is sped up by tensile surface residual stresses. However, compressive surface residual stresses tend to keep cracks closed and help reduce their propagation, lengthening components useful life [Lloyd 1999].

Machining operations, among which milling can be found, tend to produce high magnitude tensile surface residual stresses and slightly compressive ones in the subsurface layer, as Li, et al. [Li 2023] reviewed. Aiming to improve fatigue behaviour, critical components are usually subjected to mechanical (shot peening, deep rolling, etc.) [Schulze 2006] or thermal (normalizing, annealing) [Singh 2020] treatments that reduce tensile surface residual stresses and, in some cases, even introduce compressive ones instead.

Recent developments by Sáinz de la Maza García, et al. [Sáinz de la Maza García 2025] showed that, if machining is performed having the workpiece under an externally introduce tensile stress state, after unclamping, surface residual stresses become compressive. This machining technology was named “Prestress Assisted Machining” or PAM. The method proposed in this work is directly based on the technique studied by Sáinz de la Maza García, et al. and the results they obtained, addressing one of the proposed future research by studying non-pure-tensile prestress states. Therefore, this work expands previous research by applying PAM with bending stresses instead of pure tensile stresses.

2 THEORETICAL BASIS

Machining under external prestressing loads is a novel and still uncommon manufacturing technique. Thus, in this section, the theoretical principles that explain the usefulness of the method are summarized.

2.1 Effect of tensile force on residual stresses

The main point of milling under externally introduced prestresses is achieving high surface integrity on machined parts, assuring compressive surface residual stresses that tend to reduce fatigue crack propagation.

As Sáinz de la Maza García, et al. [Sáinz de la Maza García 2025] proposed, when studying prestressing effects on machined surfaces, modelling the workpiece as a two layered element is adequate. When milling, a thin layer near the fresh-machined surface gets affected by the machining process, while the rest of the workpiece does not suffer any machining induced change. Therefore, if the workpiece is prestressed, the bulk material, is subjected to prestressing stresses, but the surface layer, due to heat generation and plastic deformation, is under machining induced residual stresses.

Once the machining operation is completed, prestressing loads are removed and the bulk material, unaffected by milling, tends to recover its initial geometry. Bulk material recovery pulls the surface layer to deform with it. Considering that the machining affected layer is generally much thinner that the workpiece, this introduces a residual stress state that may be estimated as the initial, machining induced residual stresses minus the prestressing stresses in the material volume of the machined surface layer.

Consequently, if prestressing loads are tensile, final residual stresses are compressive, while initial compressive prestressing loads tend to produce tensile surface residual stresses. To reduce fatigue issues, introducing compressive residual stresses is pursued.

Sáinz de la Maza García, et al. [Sáinz de la Maza García 2025] also proposed that when only one side of the workpiece is milled, as compressive residual stresses are not symmetrical, the final workpiece tends to bend, producing geometrical error. Although this may be a problem for final components, during this research, this effect was seen to be negligible.

2.2 Using bending loads instead of pure tensile forces on thick workpieces

As exposed, if compressive surface residual stresses are pursued, introducing pure tensile prestressing loads would be the most straightforward solution. However, although this method is valid for thin components, as thickness and material section are increased, needed force easily becomes too high and requires large mechanical or hydraulic systems to prestress the component, being manual prestressing (using a mechanical vise) with tensile forces highly limited.

When component geometry is slender, even if thickness is significant, using traverse loads to bend it requires much lower forces than stretching it with longitudinal loads. When a workpiece is bent, it is well known that from the neutral fibre towards the external surface of the curve, material is subjected to tensile stress, while under the neutral fibre, stress is compressive. Thus, if in a thick workpiece PAM is to be performed in low depth milling operations, using bending loads and machining the outer surface is easier and requires less robust fixtures than using pure tensile forces. A possible fixture for this method is represented in Fig. 1, where a rather thick but slender workpiece is bent against a cylindrical curved surface of radius *R* using two traverse forces *F* and a shallow milling operation is performed.

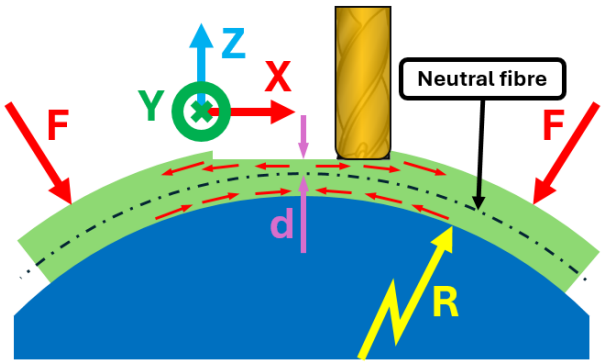

Fig. 1: Stresses introduced by bending loads for slender workpiece machining.

In this situation, longitudinal stress σ_{xx} is calculated as shown in Equation (1) [Alcaraz 2012], where *E* represents Young's modulus, ε_{xx} is the unit deformation, *d* is the distance of the study point respect to the neutral fibre and *R* is the radius of curvature in the study section. It must be pointed out that in this work, the radius of curvature used for calculation is that of the fixture (represented in Fig. 1) as workpiece thickness is much smaller than R, but the radius to be considered is that of the studied material point. Small deformation hypothesis is used, as expected deformations are significantly smaller than workpiece dimensions.

$$\sigma_{xx} = E * \varepsilon_{xx} = \frac{E*d}{R} \quad (1)$$

Note that if the two layered model (surface affected by milling and bulk material not affected) is valid, final residual stresses in the longitudinal (X) direction can be calculated as the initial machining induced residual stress minus the value of σ_{xx} calculated using Equation 1 for the distance *d* of the fresh machined surface and subsurface to the neutral fibre. In Z direction, normal to the machined surface, residual stress is zero (plain stress case) and in Y direction, in the surface but normal to the bending plane, residual stresses are not affected by the prestressing. If fully compressive residual stresses were pursued in the fresh surface, a spherical bending (in XZ and YZ planes) instead of a cylindrical bending (only in XZ plane), as considered for the theoretical explanations and used during the experimental testing of this work, should be chosen.

In addition to that, the needed bending momentum M_y to achieve that longitudinal stress is calculated using Equation (2) [Alcaraz 2012], in which I_y is the workpiece section moment of inertia. Equations (1) and (2) show that longitudinal tensile stress and bending momentum are inversely proportional to the bending radius.

$$M_y = \frac{E*I_y}{R} \quad (2)$$

2.3 Clamping system design

To experimentally test the usefulness of this method, a clamping system capable of introducing bending loads was designed. Theoretical considerations towards a valid fixture for testing are summarized hereafter.

The simplest method to bend slender stripes is performing a three-point bending, using two fixed supports on one side of the workpiece and a moving one in the opposite side, as illustrated in Fig. 2. Three-point bending is extensively used in sheet metal forming and in material testing, as standardized by ISO 178 [ISO 2019] among others.

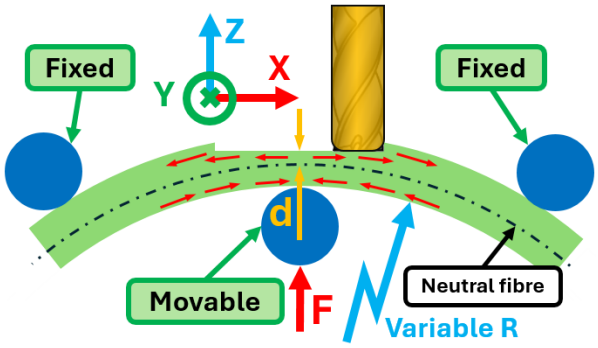

Fig. 2: Three-point bending for pocket milling.

However, this method leads to non-constant bending momentum along component length, varying linearly from 0 in both ends to a maximum value of *F*L/4* in the middle section, where *F* is the applied force in the middle section and *L* the distance between both supports [Alcaraz 2012].

During machining, ideally the complete milled area should be subjected to the same stress level, easing the generation of uniform compressive residual stresses. Therefore, as bending momentum is inversely proportional to bending radius *R*, if the whole machined area is subjected to an equal radius bending, bending momentum and thus, externally applied stress, are uniform in the machined area.

Fig. 3 shows using finite element simulation that, as expected, if workpiece is bent using a uniform radius, stresses are equal in all sections (except for both ends where the clamping is performed). It is also shown that in the neutral fibre, stress is zero, whilst in the outer surface,

tensile stress is maximum and in the inner surface, stress is compressive. Due to contact with the curved fixture, local differences appear in the inner surface.

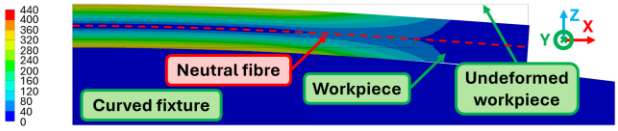

Fig. 3: Bending induced stress simulation for a 10 mm thick aluminium alloy workpiece using a 1000 mm radius curve fixture (considering perfectly elastic behaviour).

Based on the previous considerations, the fixture shown in Fig. 4 was designed. It has six clamping surfaces with different radii (flat, 4000 mm, 2000 mm, 1000 mm, 500 mm and 300 mm) that allow manufacturing different thickness components with various stress levels. Note that in this work, 300 mm curvature radius surface was not used (it is designed for thinner specimens and for different material workpieces) and the flat surface allows comparing results of non-prestressed machining with those milled under bending loads with a similar clamping method.

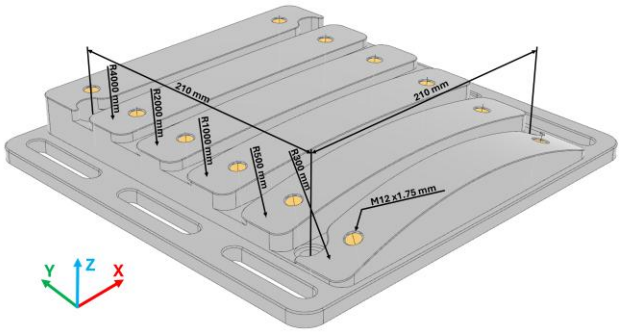

Fig. 4: Geometry and main dimensions of the designed fixture for machining under bending loads.

Fixture external geometry was designed to allow easy in-machine mounting and four holes were drilled in a 210 mm side square to allow mounting the fixture on top of a Kistler 9255B dynamometric table for measuring forces. In all clamping surfaces, two M12 threaded holes were machined to allow clamping and prestressing specimens using a bolted connection, as shown in Section 3.5.

The main advantage of using this fixture is that not only keeps a uniform stress state in the whole machining length, but it also assures that applied stress is always the same for a certain workpiece thickness and curvature radius at each depth from surface, without needing to measure it. In terms of applied prestress, the proposed system is also insensible to bolt tightening torque as long as the workpiece is in contact with the fixture in the whole machined length.

3 EXPERIMENTAL TESTING

To verify if theoretical results agree with machining results, in this section, performed experimental tests main parameters are presented.

3.1 Specimen geometry and material

During experimental testing, to achieve comparable results, all tests were performed using the same testpiece geometry and material. Specimens were manufactured using wire EDM from a single Al5083 aluminium alloy slab. A 210 x 30 mm rectangular shape was selected, with two different thicknesses: 4.5 and 10 mm. In both ends, a 15 mm wide and 27.5 mm long centred slot was cut to let tightening bolts pass through the specimens, as shown in Fig. 5.

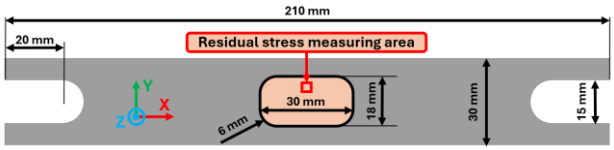

Fig. 5: Machined pocket geometry (different depths) and residual stress measuring area.

Material Young's modulus is approximately of 71 GPa, yield stress of 145 MPa and ultimate stress of 190 MPa. No significant residual stresses were initially present.

3.2 Performed tests

To study the effect of bending the workpiece during machining, and to analyse the predictability of the final residual stresses, different depth pockets were milled in multiple thickness specimens under different curvature radii. The main parameters of performed tests are summarized in Tab. 1. Note that these tests were repeated twice, and in all of them, low differences were identified (below a 10 %). Therefore, results shown in this work correspond to the average value of both equal tests, considering small differences as due to experimental errors.

Tab. 1: Performed tests parameters.

Testpiece	Workpiece thickness [mm]	Pocket depth [mm]	Curvature radius [mm]
1	10	3	-
2	10	3	2000
3	10	3	1000
4	4.5	1.5	-
5	4.5	1.5	500
6 (Shallow)	10	1	1000
6 (Deep)	10	7	1000
7	10	3	4000

In testpiece number 6 two pockets were machined, one over the neutral fibre (named "6 (Shallow)") and the other under the neutral fibre (named "6 (Deep)"). The former is comparable with every other test, while the latter aims at studying if the proposed theoretical explanation is plausible, adding a different situation in which the prestressing is expected to introduce tensile residual stresses instead of compressive.

Fig. 5 shows machined pocket geometry plan view, which was kept the same in all tests; a 30 x 18 mm rectangular pocket with 6 mm radius rounded edges. It also shows the residual stress measurement location, which was positioned in the centreline of a machining path pass to avoid irregularities between passes.

In relation to performed tests, the main characteristics that represent the theoretical effect of bending during machining are both the maximum introduced longitudinal stress (in the upper and lower surfaces) and the prestress in the fresh machined surface material before workpiece is unclamped. These stress values are summarized for each test in Tab. 2. Note that in prestressed tests, externally introduced stress in the machining affected material volume is tensile in all cases except for deep pocket of specimen 6, meaning that, as exposed in Section 2.2, expected residual stresses are compressive in all prestressing cases but one.

In Tab. 2, all stresses are calculated considering a perfectly elastic material behaviour, but as testspieces 2, 3, 5 and 6 surpass material yield stress, initial specimen surfaces suffer plastic deformation and thus, real stresses are of a lower magnitude. Combining some tests where plastic deformation was expected with others under yield point,

allowed understanding if the proposed method to estimate final residual stresses is valid when omitting plastic deformation effects. This also allowed increasing the prestressing stress in the fresh machined surface depth to study a broader variety of cases.

Tab. 2: Externally introduced stresses considering perfectly elastic behaviour (real stresses over yield stress have a lower magnitude).

Testpiece	Maximum stress [MPa]	Machined depth stress [MPa]
1	0	0
2	177.5	71
3	355	142
4	0	0
5	319.5	106.5
6 (Shallow)	355	284
6 (Deep)	355	-142
7	88.75	35.5

3.3 Cutting tools and conditions

All tests were performed using three-toothed 6 mm diameter uncoated HSS-Co8 flat-end mills. Cutting edge geometry was optimized for aluminium alloys and helix angle was of 30º.

To ensure comparable results, cutting parameters were also kept equal in al tests: a cutting speed of 170 m/min and a feed per tooth of 0.011 mm (9000 rpm spindle speed and 300 mm/min feed). Pockets were machined in depth steps of 1 mm for tests performed in 10 mm thick specimens (tests 1, 2, 3, 6 and 7) and 0.75 mm for tests 4 and 5 in thinner specimens.

3.4 Measured variables

Based on previous research results and theoretical expectations, during experimental testing a few variables were measured and studied;

- pocket floor residual stresses
- cutting force
- pocket floor roughness
- specimen plastic deformation

Considering previous tests, to characterize surface residual stresses, X-Ray diffraction (XRD) technique was chosen. This method gives accurate and easily comparable measurements, however, unlike ASTM E837-20 [ASTM 2020] hole-drilling, XRD gives only surface measurements, not full residual stress profiles. According to Sáinz de la Maza García, et al. [Sáinz de la Maza García 2025], as machining induced residual stresses are only seen in a thin surface layer, prestressing effects are limited to the surface, and thus, using XRD is adequate to study the effect of prestressing.

Cutting forces were measured using a Kistler 9255B dynamometric table located under the fixture, as detailed in Section 3.5.

Both roughness and pocket geometry measurements were carried out optically using an Alicona Infinite Focus G5 microscope. This technology was also used to verify tools geometry. However, as explained in Section 4.1, it was seen that specimens suffered significant plastic deformation, so, geometry analysis was complemented with back-surface profile measurements using a Mitutoyo Formtracer SV C3200 profilometer.

3.5 Experimental setup

Having designed the fixture and bearing in mind that machining forces were to be measured, the experimental setup shown in Fig. 6 was used for all tests. The fixture was mounted on top of the dynamometric table using four screws through the holes prepared specially for this kind of setup. Testpieces were later clamped, and bent in prestressed test cases, by means of bolt and thick washer, as shown in Fig. 6 for a non-prestressed specimen.

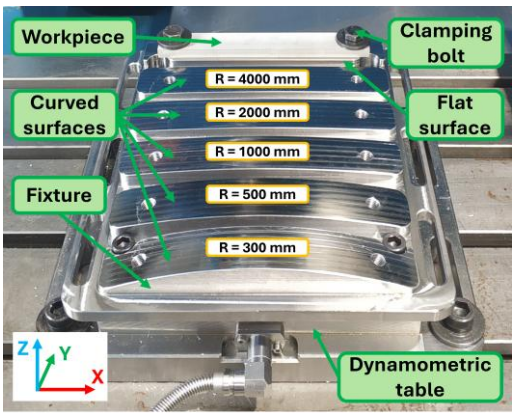

Fig. 6: Experimental setup for machining slender workpieces under bending loads.

All tests were carried out in a high-speed 3-axis Kondia HS1000 machining centre. However, manufacturing the designed fixture required a bigger and 5-axis machine, so it was milled in an Ibarmia THR-16 Multiprocess large-scale machining centre. The material used for the fixture was a 45 HRC 56NiCrMoV7 die steel.

4 RESULTS AND DISCUSSION

4.1 Geometry errors

After machining and unclamping, testpieces showed significant deformation due to local plastic deformation during bending process. This result agrees with theoretical expectations, as specimens 2, 3, 5 and 6 were intended to surpass yield stress in the unmachined surface, while testpieces 1, 4 and 7 did not reach such high stress and virtually no plastic deformation was measured after unclamping. Fig. 7 summarizes initial curvature during machining and final deformation of specimens after unclamping. *Rt* represents the theoretical radius of curvature (while clamped) and *Rr* the real measured value after unclamping. It can be seen that specimens 3 and 6, which both were bent using the same radius and their thickness is equal, showed similar behaviour.

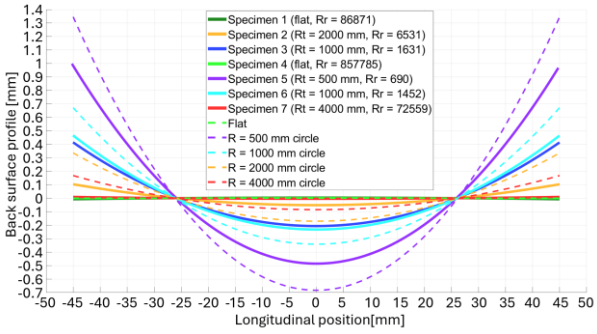

Fig. 7: Workpiece bending during machining and measured residual deformation.

In Fig. 7, each specimen is described by a real radius of curvature, as it was seen that measured profiles fitted almost perfectly a circle. This result is consistent with theoretical expectations as all study sections were curved with the same radius of curvature, and thus, surpassed by the same amount material yield point (same relation

between prestressing elastic and plastic deformation in all sections). This deformation leads to non-flat workpieces, so, for real workpieces, it is not admissible. However, as it is due to intentionally surpassing material yield stress, for real components, it could be avoided by keeping stress levels in every point of the material under its yield point, as done, for example, in specimen 7.

Locally, in machined pocket floors, another geometrical error was found; as pockets were machined using a front end mill, and during material removal, bending stresses tend to slightly modify pocket floor geometry (due to elastic deformation recovery), small magnitude depth changes were seen between machining paths (in the order of 10 µm). Additionally, in relation to the geometric errors, pocketing operations were performed using a flat end mill in a 3-axis machine, and therefore, no correction was made to the bottom surface to compensate introduced curvature, easing the testing stage. However, for industrial application, this effect should be compensated using 5-axis pocketing that keeps the tool always perpendicular to the curved surface of the workpiece.

4.2 Residual stresses

Analysing residual stress measurements, non-prestressed tests (tests 1 and 4) showed low magnitude compressive surface residual stresses in both X and Y directions. Although it is common for milling to generate tensile residual stresses, depending on cutting parameters, this result is possible, and prestressing should increase the compressive residual stress magnitude.

As theoretically exposed in Section 2.2, experimental results show no meaningful differences in Y direction stresses when machining under bending loads. In longitudinal direction, however, thanks to external prestressing, residual stresses were seen to be much more compressive in most tests. In the deep pocket of testpiece 6, as expected, final residual stresses were tensile and of a significant magnitude (about 50 MPa). Fig. 8 summarizes all residual stress measurements (green crosses). Experimental measurements of testpiece 7 showed values greater than yield stress, and away from expected results, which point towards a measurement issue. Therefore, residual stress measurement of testpiece 7 should be ignored.

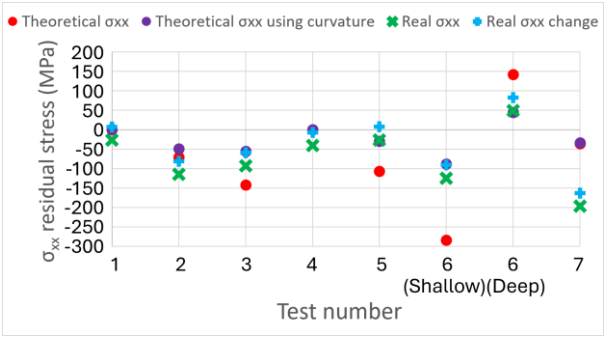

Fig. 8: Calculated and measured machined surface residual stresses.

The main goal of this research, considering the previous evidences of the usefulness of Prestress Assisted Machining [Sáinz de la Maza García 2025], was to verify if using simple theoretical estimations of final residual stresses was accurate enough to determine needed prestressing loads. As proposed in Section 2.2, theoretical residual stresses in X direction can be calculated using Equation 1. Theoretical results using that equation are also plotted in Fig. 8 as red dots. However, these calculations result in the change in residual stresses considering a perfectly elastic behaviour except in the surface layer. To determine the change in residual stresses instead of the absolute value, in Fig. 8, blue plus signs show experimental measurements minus the non-prestressed tests average residual stress. Finally, as real specimens suffered elastic and plastic deformations, to make both datasets comparable, plastic deformation effect must be taken into account in theoretical calculations. To achieve this, purple dots in Fig. 8 were obtained substracting to the original theoretical values, results of Equation 1 considering the final specimens curvature radii (Rr in Fig. 7) as radius of curvature.

Fig. 8 shows clear evidence of agreement between theoretical expectations once plastic deformations were taken into account (purple dots) with measured residual stress variation (blue plus signs). This means that performing a simple, non-prestressed test and measuring machining induced surface residual stresses, using Equation 1, of great simplicity, final prestressed residual stresses can be effectively calculated. Therefore, if a certain surface residual stress value is to be obtained, the needed radius of curvature can be calculated and used for machining to obtain a high surface integrity component without needing to perform further postprocessing operations (minimum radius of curvature is limited by plastic deformations).

In short, experimental tests showed that using the proposed method, if plastic deformation is avoided or predicted, final machining induced surface residual stresses can be effectively controlled.

4.3 Effect on cutting forces

Sáinz de la Maza García, et al. [Sáinz de la Maza García 2025] investigated the effect of machining under external tensile prestress on cutting forces, but no clear results were obtained for the performed tests. However, for certain machining operations and cutting conditions in some materials, it could be expected to find lower cutting forces when prestressing. Material removal is performed by surpassing material ultimate stress, and prestressing induces an initial stress state closer to the ultimate stress, meaning that lower forces could be needed to perform material removal.

To study the effect of bending loads on cutting forces, Fig. 9 summarizes measured forces for tests 4 (non-prestressed) and 5 (prestressed). For clearness, the rest of the tests (with different number of passes) are not shown, but similar tendencies can be identified, although differences are of a lower magnitude. Values shown in Fig. 9 are smoothed using a moving average filter to hide high frequency variations (due to tooth passing frequency) and clearly identify force tendency.

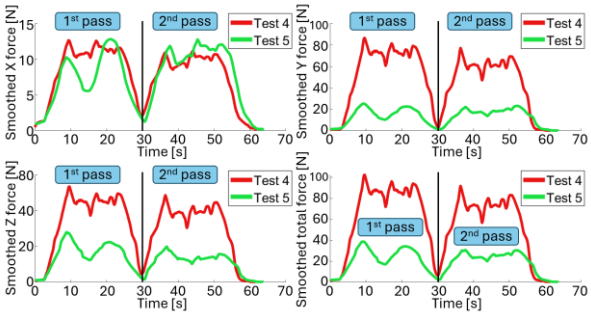

Fig. 9: Smoothed measured forces for tests 4 (non-prestressed) and 5 (prestressed).

Two depth passes are clearly seen in Fig. 9; the former shows slight differences in force evolution shape between

both tests (due to the initial, unmachined surface curvature), however, the latter exhibits very similar tendencies but with different force magnitudes. Thus, although both passes force is similar and may be used to compare prestressing and non-prestressing tests, using the second pass gives a more robust validation of the force reduction when prestressing.

According to these results, it is evident that, for some cases, the behaviour predicted by Sáinz de la Maza García, et al. [Sáinz de la Maza García 2025], where cutting force is reduced by prestressing, can be found. In performed tests, when machining under externally introduced bending loads, forces were significantly lower than in non-prestressed machining. Between tests 4 and 5, cutting force was reduced by approximately a 65%, as a consequence of having the removed material at a high stress state, near its ultimate stress, and the machining operation needed to increase that stress less than without prestressing in order to cut material.

4.4 Surface roughness

Unlike with pure tensile prestress (as Sáinz de la Maza García, et al. [Sáinz de la Maza García 2025] proposed), using bending loads, the workpiece is clamped against a fixture in contact with it all along the machining length. Therefore, it was expected to see low improvement on surface roughness during performed tests. However, bending loads also modify workpiece natural frequencies, and in consequence, the tendency to vibrate. It was found that test 2 and the shallow pocket of testpiece 6 showed higher roughness than flat tests. However, all the other tests showed a significant improvement, reaching a 70% roughness reduction in some cases.

In average, prestressed tests showed a 20% reduction in Ra average roughness parameter and an 18% reduction in Rz maximum roughness height parameter.

These results are reasonable, as both tests where roughness increased showed chatter marks; prestressing moved natural frequencies closer to tooth passing frequency. In every other test, natural frequencies were modified to avoid tooth passing frequency better than non-prestressed flat milling tests.

5 CONCLUSIONS

Pocket milling under external bending prestress, using the proposed fixture design, showed clear improvements in surface residual stresses and machining forces. However, during experimental testing, plastic deformations were seen. As using higher curvature radii (big enough to avoid plastic deformations) improvement was seen to be of a similar magnitude, the proposed method could be used in real components under lower bending loads than those used during the tests to analyse the method, avoiding plastic deformations.

It was also verified that prestressed machining using bending loads can effectively control workpiece tendency to vibrate during milling. Furthermore, machining bent workpieces showed a promising reduction in both cutting force components normal to the main prestressing direction and in the total force.

Finally, applying uniform prestressing at a certain depth below the surface was seen to need significantly lower prestressing forces than using pure tensile stresses, which opens the path towards PAM of thicker workpieces.

6 FUTURE RESEARCH

Considering the results and limitations of this work, continuing the research on prestressed machining under bending loads is highly encouraged. Some geometry errors are easily avoidable by reducing the maximum external stresses or by changing workpiece material, while the others, imply tool path corrections or different machining operations, such as 5-axis pocketing. The use of this method for ball-end mill copying operations is expected to give significantly better results that pocket milling, because of the lower depth of cut and because using ball-end mills would need to compensate machining paths using the fixture curvature but, unlike with end mills, gouging is avoided. Furthermore, this research was limited to thicker specimens to those machined under tensile prestressing in previous works, but as needed external forces are of a lower magnitude, future works should cover the effect of machining even thicker components under bending loads using larger curvature radii.

7 ACKNOWLEDGMENTS

Regarding data analysis, the project was performed with the help of AIMS Unit (Artificial Intelligent Manufacturing for Sustainability) at the University of the Basque Country (UPV/EHU). Thanks are addressed to Basque Government, for the support of University research groups, IT1573-22. The authors acknowledge the funding support received from MICIU/AEI /10.13039 /501100011033 and FEDER, UE, through project PLEC2024-011247.

8 REFERENCES

[Alcaraz 2012] Alcaraz, J. L., et al. Elasticidad y resistencia de materiales. 2012, Bilbao: Publicaciones - Escuela Técnica Superior de Ingeniería, ISBN 9788493970317

[ASTM 2020] American Society for Testing and Materials. ASTM E837-20 Standard test method for determining residual stresses by the hole-drilling strain-gage method. November 2020.

[ISO 2019] International Organization for Standardization. ISO 178:2019 Plastics – Determination of flexural properties. April 2019.

[Li 2023] Li, Y., et al. Review on residual stress and its effects on manufacturing of aluminium alloy structural panels with typical multi-processes. Chinese journal of aeronautics, May 2023, Vol. 36, No.5, pp 96-124, ISSN 25889230

[Lloyd 1999] Lloyd, J.R.T. The effect of residual stress and crack closure on fatigue crack growth. Ph. D. thesis, University of Wollongong, 1999.

[Sáinz de la Maza García 2025] Sáinz de la Maza García, A., et al. Prestress Assisted Machining: Achieving high surface integrity in thin wall milling. Results in Engineering, June 2025, Vol. 26, ISSN 2590-1230

[Schulze 2006] Schulze, V. Modern mechanical surface treatment. 2006, Wiley-VCH, ISBN 9783527313716

[Singh 2020] Singh, R. 12 – Heat treatment of steels. In: R. Singh, ed. Applied Welding Engineering (Third edition), 2020, pp 105-118, ISBN 9780128213483